Orbital ordering and exchange interaction in the manganites

Hakim Meskine, Harald König,* and Sashi Satpathy
Department of Physics and Astronomy, University of Missouri–Columbia, Columbia, Missouri 65211

(Received 30 October 2000; revised manuscript received 9 February 2001; published 15 August 2001)

The microscopic origin of the exchange interaction in manganites is studied by solving an electronic model Hamiltonian for the Mn-O-Mn triad. It is shown that the magnetic structure of $La_{1-x}Ca_xMnO_3$ is correctly described within an electronic Hamiltonian model, provided that the appropriate orientation of the $Mn(e_g)$ orbitals induced by the Jahn-Teller effect is taken into account. The Jahn-Teller distortions of the MnO_6 octahedra control the orientation of the e_g orbitals in the crystal, which in turn is shown to determine the sign of the magnetic exchange. Electron hopping involving the $Mn(t_{2g})$ orbitals is found to be important in certain situations, for instance, it can cause a sign change in the exchange interaction, from ferromagnetic to antiferromagnetic, as a function of the Mn-O-Mn bond angle. All our results are obtained by exact diagonalization of the model Hamiltonian, either by direct diagonalization or by diagonalization using the Lanczos method, if the Hamiltonian is too big, and are rationalized using results of the fourth-order perturbation theory. The exchange interactions (signs and magnitudes) of the end members $LaMnO_3$ and $CaMnO_3$ as well as of the half-doped compound, $La_{1/2}Ca_{1/2}MnO_3$, are all described correctly within the model.

DOI: 10.1103/PhysRevB.64.094433 PACS number(s): 75.30.Et, 75.30.Vn, 72.80.Ga

I. INTRODUCTION

The magnetic phase diagram of the colossal magnetoresistive manganites $La_{1-x}Ca_xMnO_3$ is quite rich because of the interplay between the charge, orbital, lattice, and spin degrees of freedom. A clear understanding of the coupling between these degrees of freedom is critical to the understanding of many of the intriguing properties of these materials including the colossal magnetoresistance.

This paper deals with the microscopic origin of the exchange interaction in the manganites. In the 1950s a set of semiempirical rules were formulated by Goodenough, Kanamori, and Anderson (GKA rules) to explain the magnetic interactions in manganites.[1–4] More quantitative calculations of the magnitudes of the exchange were attempted only recently for $LaMnO_3$ using first-principles electronic structure methods.[5,6] The two calculations, one by Solovyev *et al.*[5] employing the density-functional method and the other by Su *et al.*[6] employing the *ab initio* Hartree-Fock method, produced conflicting results even for the signs of the exchange interactions. The interplane Mn-O-Mn exchange for $LaMnO_3$ obtained in Ref. 5 is in fact ferromagnetic in direct contradiction with the GKA rules. In view of this, it is important to examine the magnetic exchange in manganites.

The approach in this paper is to understand the origin of the magnetic exchange from the solution of a simple, minimal model. The Hamiltonian model is simple enough that it can be solved exactly. The needed electronic parameters are taken with guidance from the *ab initio* density-functional results.[7–9]

It is shown that within an electronic Hamiltonian model, the magnetic exchange in the $La_{1-x}Ca_xMnO_3$ system can be described correctly, if one takes into account the appropriate Jahn-Teller splitting of the e_g orbitals induced by the coupling to the MnO_6 octahedra. The model not only describes correctly the exchange interactions in $LaMnO_3$, but also in the other two members in the $La_{1-x}Ca_xMnO_3$ series, viz., $CaMnO_3$ and $La_{1/2}Ca_{1/2}MnO_3$. Thus the model correctly describes the type-*A*, type-*G*, and type-CE magnetic structures (Fig. 1) observed in $LaMnO_3$, $CaMnO_3$, and $La_{1/2}Ca_{1/2}MnO_3$, respectively.[10–12] In addition, we show that the electron hopping involving the $Mn(t_{2g})$ orbitals adds a net ferromagnetic component and in certain situations it re-

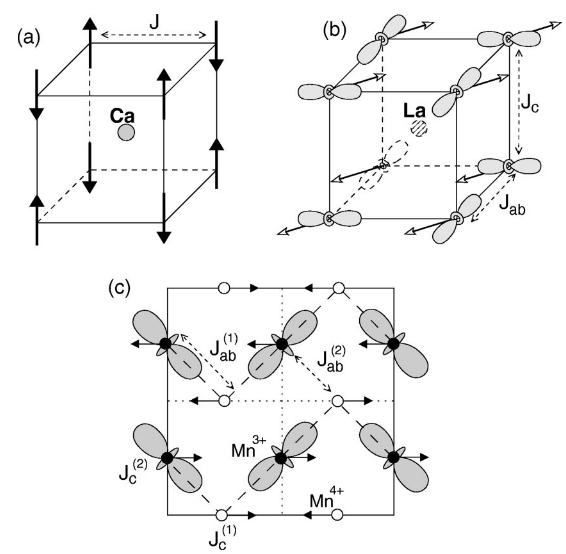

FIG. 1. Magnetic and orbital ordering in the type-*G* (a), type-*A* (b), and type-CE (c) structures observed in $CaMnO_3$, $LaMnO_3$, and $La_{1/2}Ca_{1/2}MnO_3$, respectively. In the CE structure, the basal (ab) planes are stacked one over the other, along the *c* direction with the Mn spins reversed on the successive planes. The dashed lines in (c) indicate the ferromagnetically coupled zigzag chains of Mn atoms. The *J*'s indicate the magnetic exchange between the Mn atoms: $J_{ab}^{(1)}$ and $J_{ab}^{(2)}$ are the intraplanar exchange interactions, while $J_c^{(1)}$ and $J_c^{(2)}$ denote the interplanar interactions, along bonds perpendicular to the plane of paper. Arrows indicate magnetic moments on the Mn atoms.

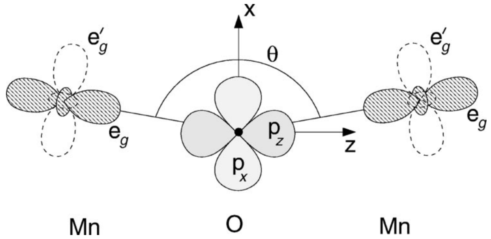

FIG. 2. The Mn-O-Mn triad considered in the paper and the nomenclature for the different orientations of the Mn(e_g) orbital. The z^2-1 orbital oriented along a Mn-O bond is referred to as the e_g orbital, while the ones perpendicular to it are referred to as e_g' or e_g''. The e_g' orbital lies on the plane of the figure as shown while the e_g'' (not shown) lies perpendicular to the plane. The corresponding counterparts forming the two-dimensional manifold of the Mn(e_g) orbitals are denoted by E_g, E_g', or E_g''. Thus if $e_g = z^2-1$ in a certain coordinate system, then $E_g = x^2-y^2$ and so on. The y axis is normal to the plane of the triad.

verses the sign of the exchange interaction as the Mn-O-Mn bond angle is varied.

II. THE HAMILTONIAN AND ITS PARAMETERS

Consider two MnO_6 octahedra sharing a common vertex via an oxygen atom as is encountered in the manganites. The bond angle of the Mn-O-Mn triad is 180° in the ideal perovskite structure but deviates somewhat from this ideal value in the actual crystal. Since the manganites are mixed valence systems consisting of Mn^{3+} and Mn^{4+} ions, with electronic configurations of $t_{2g}^3 e_g^1$ and $t_{2g}^3 e_g^0$, respectively, we can have any of the three combinations of Mn valence on the triad, viz., Mn^{3+}-O-Mn^{3+}, Mn^{4+}-O-Mn^{4+}, and Mn^{3+}-O-Mn^{4+}. These are found in the three compounds $LaMnO_3$, $CaMnO_3$, and $La_{1/2}Ca_{1/2}MnO_3$, respectively.

Now, the Mn^{3+} being a Jahn-Teller ion, the oxygen octahedron surrounding it is distorted, with the result that the degeneracy of the e_g orbitals is removed. The orbital with the lower energy is a "z^2-1"-type orbital with its lobes pointed towards the longest Mn-O bond. This is sometimes referred to as the "long" cation-anion bond, while the rest of the Mn-O bonds within the MnO_6 octahedron are the "short" bonds. The orientation of the occupied "z^2-1" orbital is along the Mn-O bond if it is long, or else the orientation is perpendicular to it, if the bond is short.

The orientations of the Mn and the oxygen orbitals are illustrated in Fig. 2. The orbitals explicitly considered here are the three O(p) orbitals and the five Mn(d) orbitals. Because the e_g orbitals are partially occupied in Mn^{3+} and since the electronic hoppings for the two orbitals are different, the magnetic exchange will depend on which of these two orbitals is occupied.

Keeping this in mind, we introduce the nomenclature of e_g, e_g', or e_g'', for the occupied e_g orbital in Mn^{3+}, depending on how it is oriented with respect to the Mn-O bond in the triad as shown in Fig. 2. The e_g orbital is a z^2-1-type orbital with the z axis along the Mn-O bond. The e_g' is a similar z^2-1-type orbital except that now the z axis is on the plane of the Mn-O-Mn triad and perpendicular to the Mn-O bond. The e_g'' is oriented perpendicular to both e_g and e_g' just defined. It is however not relevant to the present case since the e_g'' orbital orientation is not found in the compounds under study here. The remaining orbital of the two-dimensional manifold will be called E_g, E_g', or E_g''. E_g, for instance, denotes the x^2-y^2 orbital, with z axis along the Mn-O bond. The y axis is chosen to be normal to the plane of the triad.

It turns out that the orientation of these e_g orbitals, in case of the Mn^{3+} atom, will have a direct bearing on the magnetic coupling.[13,14] For this reason, even though the oxygen atoms forming the MnO_6 octahedra around the Mn atoms are not explicitly considered in our Hamiltonian, the Jahn-Teller splittings of the e_g orbitals induced by the distortions of the MnO_6 octahedra are taken into account properly.

With these considerations, the Hamiltonian for the Mn-O-Mn triad is written as

$$\mathcal{H} = \mathcal{H}_{\mathrm{KE}} + \mathcal{H}_{\mathrm{Coulomb}} + \mathcal{H}_{\mathrm{Hund}}, \tag{1}$$

where the three terms are, respectively, the kinetic, Coulomb, and the Hund's-rule energies,

$$\mathcal{H}_{\mathrm{KE}} = \sum_{i\nu}^{\mathrm{O}} \epsilon_p n_{i\nu} + \sum_{i\alpha\nu}^{\mathrm{Mn}} \epsilon_d(\alpha, Q_i) n_{i\alpha\nu} + \sum_{\langle ij\rangle \alpha\beta\nu} t_{i\alpha,j\beta}(c_{i\alpha\nu}^\dagger c_{j\beta\nu} + \mathrm{H.c.}), \tag{2}$$

$$\mathcal{H}_{\mathrm{Coulomb}} = \sum_{i}^{\mathrm{Mn,O}} n_i(n_i - 1) U_i, \tag{3}$$

and

$$\mathcal{H}_{\mathrm{Hund}} = -J_H \sum_{i\alpha}^{\mathrm{Mn}} n_{i\alpha\uparrow} n_{i\alpha\downarrow}. \tag{4}$$

Here, i, α, ν are, respectively, the site (manganese or oxygen), orbital (the five d orbitals on Mn and the three p orbitals on oxygen), and spin indices. $\langle ij\rangle$ indicates summation over the nearest neighbors, $c_{i\alpha\nu}^\dagger$ is the creation operator, $n_{j\beta\nu}$ is the corresponding number operator, and the site occupancy $n_i \equiv \Sigma_{\alpha\nu} n_{i\alpha\nu}$.

The first term in the Hamiltonian is the kinetic energy term. The matrix elements $t_{i\alpha,j\beta}$ are the appropriate Koster-Slater tight-binding hopping integrals[15,16] between the Mn and the O atoms. As indicated from band calculations, Mn(d)-O(p) hopping is an important hopping in the problem and only this has been retained in the Hamiltonian Eq. (1). The hopping integrals between different orbitals are listed in Table I in terms of the two p-d hopping parameters $V_{pd\sigma}$ and $V_{pd\pi}$. The second term $\mathcal{H}_{\mathrm{Coulomb}}$ represents the on-site Coulomb interaction.

The last term is the Hund's-rule energy that favors parallel alignment of electron spins on the Mn site. The Hund's energy J_H is of the order of 1 eV for the Mn atom, but is often taken to be ∞ for simplicity. Sometimes a simpler version of the Hund's-rule energy is used in the literature,

TABLE I. Koster-Slater tight-binding matrix elements $\langle a|H|b\rangle$ between the oxygen p orbitals and manganese d orbitals. Here, $t=V_{pd\sigma}$, $t'=V_{pd\pi}$, $\alpha=\cos(\theta/2)$ and $\beta=\sin(\theta/2)$. The e_g, e'_g, and e''_g (E_g, E'_g, and E''_g) orbitals have specific orbital orientation with respect to the Mn-O-Mn bond as indicated in Fig. 1 and the corresponding text.

	$\|e_g\rangle$	$\|E_g\rangle$	$\|xy\rangle$	$\|yz\rangle$	$\|zx\rangle$
$\langle x\|$	$-\alpha t$	0	0	0	$-\beta t'$
$\langle y\|$	0	0	0	t'	0
$\langle z\|$	$-\beta t$	0	0	0	$\alpha t'$
	$\|e'_g\rangle$	$\|E'_g\rangle$	$\|xy\rangle$	$\|yz\rangle$	$\|zx\rangle$
$\langle x\|$	$-\frac{\alpha t}{2}$	$\frac{\sqrt{3}\alpha t}{2}$	0	0	$-\beta t'$
$\langle y\|$	0	0	t'	0	0
$\langle z\|$	$\frac{\beta t}{2}$	$-\frac{\sqrt{3}\beta t}{2}$	0	0	$-\alpha t'$
	$\|e''_g\rangle$	$\|E''_g\rangle$	$\|xy\rangle$	$\|yz\rangle$	$\|zx\rangle$
$\langle x\|$	$-\frac{\alpha t}{2}$	$\frac{\sqrt{3}\alpha t}{2}$	$-\beta t'$	0	0
$\langle y\|$	0	0	0	0	t'
$\langle z\|$	$\frac{\beta t}{2}$	$-\frac{\sqrt{3}\beta t}{2}$	$-\alpha t'$	0	0

$$\mathcal{H}_{\rm Hund}=-J_H\sum_i^{\rm Mn}\vec{S}_i\cdot\vec{\sigma}_i, \qquad (5)$$

especially when the Mn(t_{2g}) spins are treated as classical core spins $\vec{S}$ interacting with itinerant electrons (spin $\vec{\sigma}_i$) with no hopping allowed for the t_{2g} electrons. The earlier expression Eq. (4) for $\mathcal{H}_{\rm Hund}$ allows us to treat the t_{2g} electrons as mobile with no fixed core spin. The t_{2g} hopping will be shown later to significantly contribute to the magnetic interaction in the manganites. Though not exactly identical, the two forms of the Hund's energy $\mathcal{H}_{\rm Hund}$ are analogous and describe the same physics as far as manganites are concerned.

The on-site energies, indicated in Fig. 3 for the

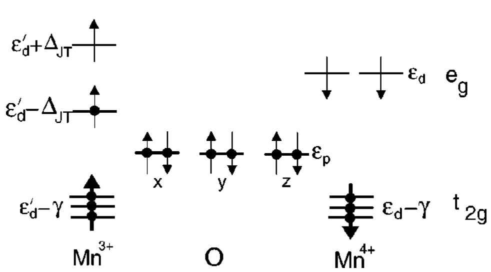

FIG. 3. Electronic configuration and one-electron orbital energies for Mn^{3+}-O-Mn^{4+}. The Jahn-Teller splitting at the Mn^{3+} site is caused by the oxygen octahedral distortion. Solid circles indicate the occupied one-electron states, while the arrows indicate the spins.

TABLE II. Typical Hamiltonian parameters for $La_{1-x}Ca_xMnO_3$ used in our calculation of exchange. Energies are in eV's. The on-site energy for oxygen p orbitals ϵ_p is taken equal to zero, while the on-site energy for the Mn(d) orbitals depends on the charge state of the Mn atom (see Fig. 3). These parameters lead to a MnO_6 p-d charge transfer energy of $\Delta_1=\Delta_2=5$ eV for both $CaMnO_3$ and $LaMnO_3$ as discussed in the text. $V_{pd\pi}$ which appears in the t_{2g} hopping is taken to be $\approx -0.46V_{pd\sigma}$ in accordance with Harrison's scaling.

ϵ_p	ϵ_d	ϵ'_d	γ	Δ_{JT}	$V_{pd\sigma}$	U_p	U_d	J_H
0	2	−5	2	1.0	1.65	3.0	6.0	1

Mn^{3+}-O-Mn^{4+} case, are given by ϵ_p and ϵ_d for the O and the Mn atoms, respectively. Note that the on-site energies $\epsilon_d(\alpha,Q_i)$, where α goes over the five d orbitals, depend on the charge state Q (Mn^{3+} or Mn^{4+}) of the Mn atom on account of the static Jahn-Teller distortion of the MnO_6 octahedra, which is present at the Mn^{3+} site but not at Mn^{4+}. Thus for the Mn^{3+} site, we have: $\epsilon_d(e_g^1,{\rm Mn}^{3+})=\epsilon'_d-\Delta_{JT}$ and $\epsilon_d(e_g^2,{\rm Mn}^{3+})=\epsilon'_d+\Delta_{JT}$, where e_g^1 and e_g^2 are the two Jahn-Teller-split e_g orbitals, with Δ_{JT} being the Jahn-Teller one-electron energy gain at the Mn^{3+} site. For the Mn^{4+} site, by contrast, we will have $\epsilon_d(e_g^1,{\rm Mn}^{4+})=\epsilon_d(e_g^2,{\rm Mn}^{4+})=\epsilon_d$, since there is no Jahn-Teller splitting there. Note that we have taken two different energies ϵ_d and ϵ'_d, for the Mn^{4+} and Mn^{3+}, respectively, since quantities such as the local Madelung potential affecting on-site energies are in general site and crystal specific. The on-site energies for the t_{2g} orbitals are taken an amount γ below the e_g energies, which represents the crystal-field splitting. The magnitudes of the ϵ_d used in our calculations were inferred from the experimental charge transfer data[17,18] and they have been listed in Table II together with other parameters.

Before we proceed to a discussion of the results, there is one more point that needs to be clarified in connection with the on-site energy $\epsilon_d(\alpha,Q_i)$. Consider, for example, the case of Mn^{4+}-O-Mn^{4+}, which occurs in $CaMnO_3$. Now, the ground state for this case will have perturbative contributions from a fermionic configuration, where a charge transfer has occurred from say the oxygen atom to a Mn atom, making it Mn^{3+}. Now, if the MnO_6 octahedron around this Mn^{3+} atom is allowed to respond to the electronic motion, the on-site Mn(e_g) energy for the added electron will be $\epsilon_d-\Delta_{JT}$, taking into account the Jahn-Teller energy gain Δ_{JT}. Else, if the octahedron is assumed to be fixed in position, the energy will simply be ϵ_d. We shall assume the latter, which is tantamount to assuming the electronic motion to be fast as compared to the lattice degrees of freedom. This is however not strictly true and the electron-lattice coupling does in fact have important consequences such as the oxygen-isotope effect.[19] This type of electron-lattice coupling, the so-called dynamical Jahn-Teller effect, has been shown to reduce the magnitude of the exchange interaction and to lead to the oxygen-isotope effect.[20,21]

The typical parameter values for $La_{1-x}Ca_xMnO_3$ that we shall use in this paper are given in Table II. The sign of the exchange [antiferromagnetic (AF) or ferromagnetic (FM)] is not sensitively dependent on the values of the parameters, so that the conclusions we derive from this work are quite robust. The magnitude of the exchange on the other hand does strongly depend on the parameters, e.g., it varies as the fourth power t^4 of the hopping parameter. In view of this, the magnitude of $t \equiv V_{pd\sigma}$ will be taken as a fitting parameter, by fitting the calculated value of J to the experimental result for $CaMnO_3$. The magnitude of t needed for this is about 1.65 eV, which is quite reasonable for the $V_{pd\sigma}$ hopping between manganese and oxygen.

To have a feel for the parameters, we compute the charge-transfer energies $\Delta_1 \equiv \Delta(Mn^{3+}-O)$ and $\Delta_2 \equiv \Delta(Mn^{4+}-O)$ from the total energy differences,

$$\Delta_1 = E(d^5p^5) - E(d^4p^6) = \epsilon_d' - \epsilon_p - 5U_p + \Delta_{JT} + 4U_d,$$

$$\Delta_2 = E(d^4p^5) - E(d^3p^6) = \epsilon_d - \epsilon_p - 5U_p + 3U_d. \quad (6)$$

In computing the charge-transfer energies above, the oxygen atoms are considered to be fixed as discussed earlier, i.e., the oxygen octahedra in the solid does not move with the fluctuation of the Mn valence. This is consistent with what might occur during experiments such as photoemission and optical conductivity measurements. From the parameters of Table II, we have $\Delta_1 = \Delta_2 = 5$ eV, which is consistent with the values deduced from photoemission[17] and optical conductivity[18] measurements. The experimental values are: $\Delta_1 \sim 5$ eV, $\Delta_2 \sim 2-3$ eV, and $t_{pd} \sim 1.5$ eV. Note that to obtain these charge-transfer energies, we need to invoke a material-dependent value for $\epsilon_d - \epsilon_p$ in Table II. In the solid such a term might originate naturally from such contributions as differences in the Madelung energy.

The ground-state energies $E_{\uparrow\uparrow}$ and $E_{\uparrow\downarrow}$ corresponding to the FM and AF alignments of the $Mn(t_{2g})$ spins are obtained either by diagonalizing the Hamiltonian Eq. (1) exactly in the fermion-configuration space or by treating the electron hopping t perturbatively using standard nondegenerate perturbation theory. If the $\mathcal{H}_{\rm Hund} = -J_H \Sigma_{i\alpha}^{\rm Mn} n_{i\alpha\uparrow} n_{i\alpha\downarrow}$ form, Eq. (4), for the Hund's energy is taken, then the FM and AF alignments are specified by the appropriate total number of the up and the down electrons $n_\uparrow$ and $n_\downarrow$ in the system. The exchange interaction J between the Mn atoms is then obtained from the difference

$$J = E_{\uparrow\uparrow} - E_{\uparrow\downarrow}, \quad (7)$$

where positive (negative) values of J indicate an AF (FM) interaction between the t_{2g} spins. Note that our J is related to J' via the equation $J = 4J'S^2$, where J' appears in the standard expression for the Heisenberg Hamiltonian $H = -2J' \Sigma_{ij} \vec{S}_i \cdot \vec{S}_j$.

For the perturbation theory results to reasonably converge we must have $t \ll \Delta E$, where ΔE is the separation of the excited state energies with respect to that of the ground state. This is not always true, so that we shall in general present the results of our exact calculations, although the perturbation-theory results will be used for general arguments.

In Fig. 4 we compare the results of the perturbation theory with the results of the exact diagonalization for the case of

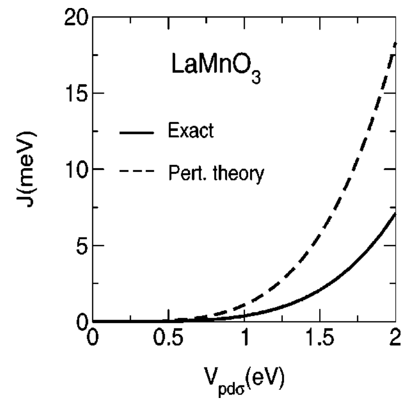

FIG. 4. Comparison of results of the perturbation theory to the results obtained from exact diagonalization for the case of $LaMnO_3$ with e_g'-e_g' orientations of the Mn orbitals. All parameters are the same as in Table II except that $J_H = \infty$.

$LaMnO_3$ with e_g'-e_g' orientations of the Mn e_g orbitals as an illustration. The perturbation theory reproduces the qualitative trend although the magnitude of the exchange interaction can be off by a factor of 2 or more depending on the parameters.

Throughout this paper, we have considered the magnetic exchange both with and without inclusion of the hopping to the $Mn(t_{2g})$ orbitals. Analytical expressions for the fourth-order perturbation theory are, however, given for the case of no t_{2g} hopping, since otherwise the expressions become quite tedious and lengthy. The full results of the perturbation theory including the effects of the t_{2g} hopping have been calculated numerically, whenever needed. Exact solution for the ground-state energies have been obtained by either the standard diagonalization method or by the Lanczos method if the size of the Hamiltonian matrix is too large.

III. EXCHANGE INTERACTION IN $La_{1-x}Ca_xMnO_3$

As shown in Fig. 1, manganites exhibit a variety of magnetic structures.[10–12] $LaMnO_3$ is a type A antiferromagnet, where the $Mn(t_{2g})$ core spins are arranged ferromagnetically within the ab planes and are aligned antiparallel between adjacent ab planes. By contrast, $CaMnO_3$ is a type G antiferromagnet, where all nearest-neighbor spins are aligned antiferromagnetically. The intermediate compound $La_{1/2}Ca_{1/2}MnO_3$ is ordered according to the CE structure, which is charge ordered and has ferromagnetic chains that zigzag in the ab plane, with identical ab planes stacked along the c direction except that the spins are reversed from one plane to another.

The Goodenough-Kanamori-Anderson (GKA) Rules. In the late 1950s Anderson,[3] Goodenough,[1,4] and Kanamori[2] developed a set of semiempirical rules that give the sign and the relative magnitude of the exchange interaction mediated by an intermediate ion. In the case of a straight Mn-O-Mn bond, these rules may be stated.

(i) When the e_g orbitals of the two cations are both partially filled with one electron each and the e_g orbitals point towards each other such that we have a large Mn-O p-d

overlap, the exchange is antiferromagnetic and comparatively large.

(ii) When the two cations have empty e_g orbitals the net exchange, mediated via the t_{2g} orbitals, is also antiferromagnetic, although its magnitude is relatively small.

(iii) When one cation has empty e_g orbitals while the other has one e_g electron, there are two scenarios: (a) If the occupied e_g orbital points towards the oxygen, so that there is a large overlap, the net exchange is ferromagnetic and moderately strong, and (b) if the occupied e_g is oriented such that its overlap with the oxygen is negligible, then we have a situation rather similar to case (ii), which leads to an antiferromagnetic exchange.

However, the GKA rules are too general and caution has to be taken to apply them to specific cases, since the sign of the exchange is controlled not just by the occupation of the orbitals but also by the relative strengths of the various electronic parameters in the system. The cancellations of the various ferromagnetic and antiferromagnetic pieces in the exchange interaction have in fact been implicitly included in formulating the above rules.

A. $CaMnO_3$

1. Exchange interaction with $J_H=\infty$ and no t_{2g} hopping

We first consider the case of $CaMnO_3$ with $J_H=\infty$ and no t_{2g} hopping. These approximations are often made for the manganites making this case worthwhile to consider. However, as will be shown shortly, the magnitude of the exchange is substantially affected by these approximations.

In $CaMnO_3$ the Mn-O-Mn triad has the nominal valence of Mn^{4+}-O^{2-}-Mn^{4+}. With t_{2g} hopping neglected, these electrons can be treated as core, and furthermore since $J_H=\infty$, the e_g orbitals with spin antiparallel to the core t_{2g} spins are not occupied. Now, retaining the O(p) and Mn(d) orbitals in enumerating the many-electron configurations accessible to the system, the total number of configurations for the FM alignment of the Mn atoms is given by ${}^nC_N\times{}^mC_M={}^7C_3\times{}^3C_3=35$ (n spin-up electrons distributed among N available spin-up orbitals and m spin-down electrons distributed among M spin-down orbitals). This results in a 35×35 Hamiltonian matrix, the size of which can be further reduced if the coordinate system is properly chosen.

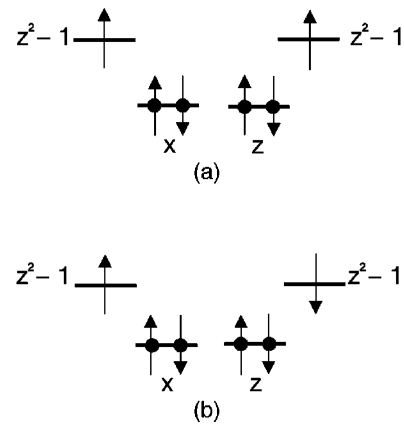

FIG. 5. Orbitals considered in forming the Hamiltonians $H_{\uparrow\uparrow}$ and $H_{\downarrow\downarrow}$ of Eqs. (8) and (9) appropriate for $CaMnO_3$. (a) corresponds to the FM alignment of the two Mn core spins while (b) corresponds to the AF alignment. Solid circles indicate states occupied by an electron.

Choosing local coordinate systems on the two Mn atoms such that the z axis points towards the oxygen atom, one finds that both the O(p_y) and the Mn(x^2-y^2) orbitals do not couple to the rest of the system. This makes the total number of configurations of a manageable size, viz., ${}^4C_2\times{}^2C_2=6$ (see Fig. 5). Taking these configurations in the following order: $|1100\rangle$,$|1010\rangle$,$|1001\rangle$,$|0110\rangle$,$|0101\rangle$, and $|0011\rangle$, where the four numbers in the ket indicate the occupation numbers for the oxygen p_x and p_z orbitals, and the e_g orbitals on the left and the right Mn atoms, in that order, the 6×6 Hamiltonian matrix is given by

$$H_{\uparrow\uparrow}=\begin{pmatrix} 6U_p & t_3 & t_4 & -t_1 & -t_2 & 0\\ t_3 & \epsilon_d+3U_p & 0 & 0 & 0 & -t_2\\ t_4 & 0 & \epsilon_d+3U_p & 0 & 0 & t_1\\ -t_1 & 0 & 0 & \epsilon_d+3U_p & 0 & -t_4\\ -t_2 & 0 & 0 & 0 & \epsilon_d+3U_p & t_3\\ 0 & -t_2 & t_1 & -t_4 & t_3 & 2\epsilon_d+U_p \end{pmatrix}. \tag{8}$$

Here, $t_1=\langle x|e_g(l)\rangle$, $t_2=\langle x|e_g(r)\rangle$, $t_3=\langle z|e_g(l)\rangle$, and $t_4=\langle z|e_g(r)\rangle$, where $l(r)$ denotes the left (right) Mn atom. Note that the above Hamiltonian is the same irrespective of which of the two forms of $\mathcal{H}_{\rm Hund}$ is used, since $J_H=\infty$.

The corresponding Hamiltonian matrix for the AF case is given by

$$H_{\uparrow\downarrow}=\begin{pmatrix} 6U_p & t_4 & -t_2 & t_3 & 0 & 0 & -t_1 & 0 & 0 \\ t_4 & \epsilon_d+3U_p & 0 & 0 & t_3 & 0 & 0 & -t_1 & 0 \\ -t_2 & 0 & \epsilon_d+3U_p & 0 & 0 & t_3 & 0 & 0 & -t_1 \\ t_3 & 0 & 0 & \epsilon_d+3U_p & t_4 & -t_2 & 0 & 0 & 0 \\ 0 & t_3 & 0 & t_4 & 2\epsilon_d+U_p & 0 & 0 & 0 & 0 \\ 0 & 0 & t_3 & -t_2 & 0 & 2\epsilon_d+U_p & 0 & 0 & 0 \\ -t_1 & 0 & 0 & 0 & 0 & 0 & \epsilon_d+3U_p & t_4 & -t_2 \\ 0 & -t_1 & 0 & 0 & 0 & 0 & t_4 & 2\epsilon_d+U_p & 0 \\ 0 & 0 & -t_1 & 0 & 0 & 0 & -t_2 & 0 & 2\epsilon_d+U_p \end{pmatrix}. \quad (9)$$

The difference in the lowest eigenvalues to the fourth order in the perturbation theory is found to be

$$J^{33}=E_{\uparrow\uparrow}-E_{\uparrow\downarrow}=\frac{4t^4\cos^2\theta}{\Delta_2^2(2\Delta_2+U_p)}. \quad (10)$$

Here and throughout the paper, the superscripts in $J^{\mu\nu}$ indicate the number of d electrons on the two Mn atoms. Thus J^{33} is appropriate for $CaMnO_3$ and J^{44} for $LaMnO_3$, and so on.

It is interesting to note from Eq. (10) that the exchange interaction has always a positive sign, since the charge transfer and the Coulomb energies, Δ and U_p, are both positive, leading to an antiferromagnetic exchange, irrespective of the magnitudes of the parameters. A similar AF interaction has been obtained earlier by Millis for a straight Mn-O-Mn bond and ignoring the degeneracy of the O(p) orbitals.[22] The results of the perturbation theory are compared to those obtained from diagonalization in Fig. 6, where the exchange interaction is shown as a function of the hopping integral. The exact results deviate from the perturbation-theory results for large hopping as expected.

2. Exchange with finite J_H

Now we relax the condition that $J_H=\infty$. The strength of the exchange is expected to diminish as J_H is reduced from infinity. In fact, it is strictly zero in the limit $J_H\rightarrow 0$, if the hopping of the t_{2g} electrons is not allowed. This is because in that case the t_{2g} electrons can be treated as core spins that are decoupled from the rest of the system, J_H being 0, and it then does not matter what the relative orientations of the t_{2g} spins are. This can be most clearly seen from the $\vec{S}\cdot\vec{\sigma}$ form of the Hund's enegy Eq. (5).

The magnitude of the Hund's-rule energy in manganites is $J_H\approx 1$ eV.[7] To illustrate the dependence of J_H on the exchange, we consider the case of $CaMnO_3$.

For simplicity, we first neglect the t_{2g} hopping, take the $\vec{S}\cdot\vec{\sigma}$ form of the Hund's enegy Eq. (5), and consider the case of the straight Mn-O-Mn bond $\theta=180°$. It then turns out that we need only consider explicitly the oxygen z and the manganese z^2-1 orbitals (six orbitals in total including spin) in the many-particle configuration, which leads to a 9×9 Hamiltonian matrix for both AF and FM cases. This can be diagonalized numerically and the results are shown in Fig. 7.

We have also obtained an expression for the exchange using the fourth-order perturbation theory, so that the functional dependence of J_H can be explicitly seen,

$$J^{33}(J_H)=\frac{4t^4}{\Delta_2^2(2\Delta_2+U_p)}+\frac{4t^4}{\Delta_2'^2(2\Delta_2'+U_p)} -\frac{2t^4}{(2\Delta_2+U_p+3J_H)}\times\left(\frac{1}{\Delta_2}+\frac{1}{\Delta_2'}\right)^2. \quad (11)$$

Here Δ_2 is the p-d charge transfer energy defined in Eq. (6) and $\Delta_2'=\Delta_2+3J_H$. Notice that our earlier result Eq. (10) is consistent with Eq. (11) in the limit of $J_H=\infty$ and $\theta=180°$.

As expected, the perturbation results show a diminishing J as J_H is decreased from infinity. This behavior is also reproduced from the exact results, shown in Fig. 7 for both forms of the Hund's energy. By contrast, if the t_{2g} hopping is allowed, there will be a difference between the ground-state energies for the FM and AF configurations even when $J_H=0$, since the t_{2g} spins are still coupled to the rest of the system via electron hopping. J thus does not go to zero for $J_H=0$, but takes a nonzero value as seen from Fig. 7.

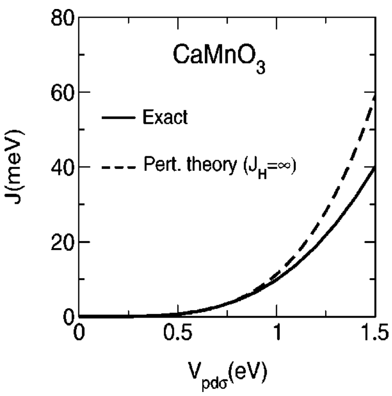

FIG. 6. Exchange interaction as a function of the p-d hopping for $CaMnO_3$ with t_{2g} hopping neglected: (a) Perturbation theory (dashed line) and (b) exact results (solid line).

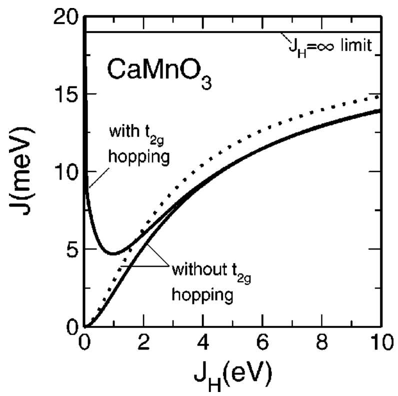

FIG. 7. Effect of a finite Hund's coupling J_H on the exchange interaction J as obtained from exact diagonalization. Both forms of $\mathcal{H}_{\rm Hund}$ are considered: (1) $\mathcal{H}_{\rm Hund} = -J_H \Sigma_i^{\rm Mn} \vec{S}_i \cdot \vec{\sigma}_i$ (dashed line) and (2) $\mathcal{H}_{\rm Hund} = -J_H \Sigma_{i\alpha}^{\rm Mn} n_{i\alpha\uparrow} n_{i\alpha\downarrow}$ (solid lines). The latter case was studied both with and without the t_{2g} hopping. Parameters are the same as in Table II except that here $V_{pd\sigma}=1.2$ eV. The figure shows three main results. (i) Both forms of the Hund's energy produce similar results when there is no t_{2g} hopping. (ii) A finite J_H ($\sim$1 eV in typical solids) significantly reduces the magnitude of J as compared to the $J_H \to \infty$ value. (iii) The t_{2g} hopping substantially affects the magnitude of exchange, if J_H is less than several eV's. Note that only the second form of the Hund's energy can be used when t_{2g} hopping is present. All three curves go to the same limit as $J_H \to \infty$ as indicated in the figure.

3. Bond-angle dependence of exchange

Figure 8 shows the bond-angle dependence of the exchange for $CaMnO_3$ and also the effect of a finite value of J_H as well as the effect of the t_{2g} hopping on the exchange. The magnitude of the exchange decreases as the angle is decreased from 180°, roughly going as $\cos^2\theta$ as suggested by the perturbation theory results Eq. (10).

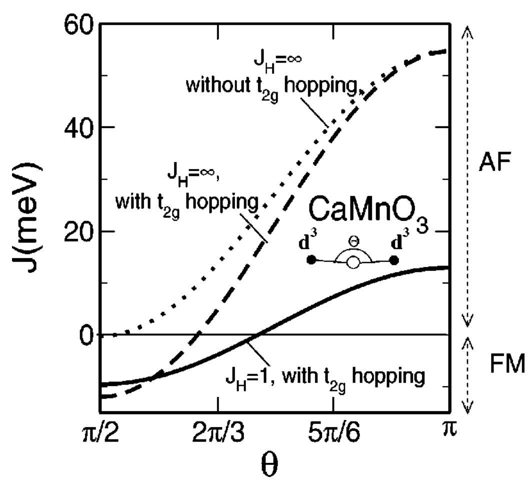

FIG. 8. Variation of the exchange interaction in $CaMnO_3$ with the bond angle θ. Shown are the results for three different cases: (a) $J_H=\infty$ and without t_{2g} hopping (dotted line), (b) $J_H=\infty$ and with t_{2g} hopping (dashed line), and (c) $J_H=1$ eV and with t_{2g} hopping (full line). Parameters other than J_H are the same as in Table II. Notice the switching of the sign of the exchange around 132° for parameters appropriate for $CaMnO_3$.

If the t_{2g} hopping is neglected, then the antiferromagnetic interaction between the t_{2g} spins in $CaMnO_3$ is caused by the subtle differences of the hopping of the O(p) electrons to the empty e_g levels. For the FM case, only three of the six O(p) electrons can hop to the Mn atoms, while in the AF case, all six electrons can participate in the hopping process. The latter case where all six electrons can hop turns out to be energetically favorable leading to an AF coupling as given by Eq. (10).

To this the t_{2g} hopping adds two competing interactions: (i) The t_{2g}-e_g hopping is ferromagnetic, because this hopping is more effective in lowering the ground-state energy, if the e_g orbital on the second Mn atom has the same spin, which in turn requires that the two t_{2g} spins be ferromagnetically aligned, and (ii) the t_{2g}-t_{2g} hopping between the occupied levels of one Mn atom and the unoccupied levels of the other is antiferromagnetic by a similar argument. In fact, if $J_H=\infty$, there is no t_{2g}-t_{2g} hopping and the former of the two competing interactions remains. This effect is seen in Fig. 8 and is in fact precisely the difference between the dotted curve and the dashed curve. The full line in that figure has all interactions and also there, J_H is taken to be 1 eV as appropriate for the manganites.

Notice also that in Fig. 8 there is a crossover between AF and FM as a function of the Mn-O-Mn bond angle θ, which is about 132° for the parameters used. The possibility of such a crossover is long known since the early work of Goodenough[12] and recently such a crossover has been experimentally observed in a somewhat different system $SeCuO_3$.[23]

The experimental $J^{\rm CaMnO_3} \approx 13.1$ meV, estimated from the Neel temperature $T_N \approx 110$ K,[10,24] agrees with the results of Fig. 6 if we take $t \equiv V_{pd\sigma} \approx 1.65$ eV. This value of t is used throughout the paper. As already mentioned, the magnitude of J is sensitively dependent on t, while the sign of the interaction is always antiferromagnetic consistent with the observed type G structure in $CaMnO_3$.

B. $LaMnO_3$

Now, we turn to the case of $LaMnO_3$, which is, unlike $CaMnO_3$, somewhat more complicated because of the three different possible orientations of the occupied e_g orbitals, depending on the specific Jahn-Teller distortion at the Mn^{3+} sites. Here, we have the nominal valence Mn^{3+}-O^{2-}-Mn^{3+}, with Mn(d^4) configurations, which can be either $t_{2g}^3 e_g^1$ if the Mn atom is on a "long" Mn-O bond or $t_{2g}^3 e_g'^1$ if the Mn-O bond is "short" (see Fig. 2). The orientation of the e_g orbitals is dictated by the specific Jahn-Teller distortion of the surrounding MnO_6 octahedra and this in turn determines the magnetic coupling.

1. Exchange interaction with $J_H=\infty$ and no t_{2g} hopping

We first discuss the case, where $J_H=\infty$ and the t_{2g} hopping is suppressed. This is important to consider because analytical expressions for the exchange can be obtained from perturbation theory in this approximation and they capture the essence of the results obtained from exact diagonalization of the full Hamiltonian like in the case of $CaMnO_3$.

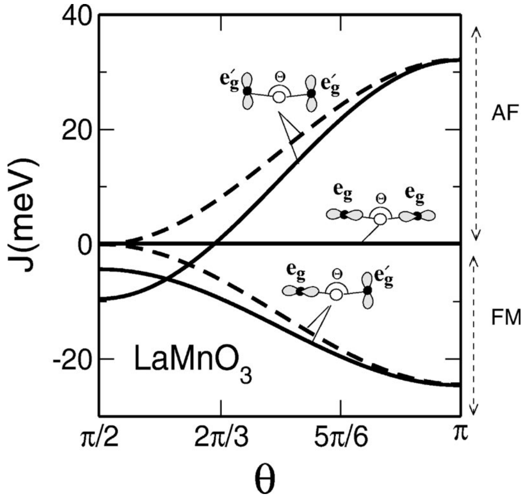

FIG. 9. Calculated exchange interaction in $LaMnO_3$ with $J_H = \infty$. The magnetic exchange is zero for the Mn (e_g-e_g) configuration in our model. The exchange interaction for the Mn (e_g'-e_g') case is antiferromagnetic, which corresponds to the case of Mn atoms located on the neighboring planes in $LaMnO_3$ along the c axis. The Mn (e_g-e_g') coupling is, by contrast, ferromagnetic as observed for the case of the Mn atoms in the ab plane. The inclusion of the t_{2g} hopping adds a ferromagnetic component to the exchange interaction as discussed in the text. In the case of the e_g'-e_g' orientation, the t_{2g} hopping leads to an exchange interaction which changes from ferromagnetic to antiferromagnetic as the angle θ is varied. Solid (dashed) lines are with (without) t_{2g} hopping included.

When the core t_{2g} spins in the Mn atoms are ferromagnetically aligned, there are six spin-up orbitals [the two e_g orbitals on each of the Mn atoms and $O(p_x)$ and $O(p_z)$] and two spin-down orbitals [$O(p_x)$ and $O(p_z)$] to be occupied by four spin-up electrons and two spin-down electrons, leading to a fifteen-dimensional ($^6C_4 \times {}^2C_2$) configuration space. Notice that neither the t_{2g} nor the $O(p_y)$ electrons are counted since they are effectively uncoupled to the rest of the system. Similarly, for the antiferromagnetic alignment of the Mn core spins, there are four spin-up and an equal number of spin-down orbitals to be occupied by three spin-up and the same number of spin-down electrons, leading to a sixteen-dimensional ($^4C_3 \times {}^4C_3$) configuration space. The exact results are obtained by simply diagonalizing these matrices and taking the difference in the ground-state energies as per Eq. (7). The exchange energy thus obtained is plotted in Fig. 9 for the three different cases of the relative orientations of the Mn(e_g) orbitals.

The expression for the exchange energy obtained from perturbation theory applicable to the Mn(d^4)-O-Mn(d^4) situation in $LaMnO_3$ is given by

$$J^{44} = \frac{1}{(\Delta_1 + \Delta_{JT})^2}\left(\frac{-T_1^2}{U_d + \Delta_{JT}} + \frac{4T_2^2}{2(\Delta_1 + \Delta_{JT}) + U_p}\right), \tag{12}$$

where

$$T_1 = \sum_{p=x,z} t_{p,e_l} t_{p,E_r} + t_{p,e_r} t_{p,E_l}, \tag{13}$$

$$T_2 = \sum_{p=x,z} t_{p,E_r} t_{p,E_l}. \tag{14}$$

Here $t_{\alpha\beta}$ are the hopping parameters $\langle \alpha | H | \beta \rangle$, $e_l(e_r)$ denotes the occupied e_g orbital on the left (right) Mn atom, and $E_l(E_r)$ denotes the corresponding empty e_g orbital. The e_l and e_r orbitals can have one of the three possible, e_g, e_g', or e_g'', orientation as discussed before. T_1 and T_2, which may be evaluated using Table I, contain the dependence on the Mn-O-Mn angle θ and on the orbital orientations.

Equation (12) shows the competition between ferromagnetic first term and antiferromagnetic second term contributions to the exchange. As seen from Eqs. (13) and (14), the ferromagnetic term involves both the occupied Mn(d_{z^2-1}) as well as the unoccupied Mn($d_{x^2-y^2}$) orbitals, denoted by e and E respectively, while the antiferromagnetic term involves only the empty Mn($d_{x^2-y^2}$) orbitals. The antiferromagnetic interaction thus originates from the virtual hopping of the O(p) electrons to the unoccupied Mn(d) levels. Now, if the two Mn core spins are antiferromagnetically aligned, then O(p) electrons of both spins can hop to a Mn atom, while for the FM alignment, only one type of spin can participate in the hopping process. The energy in the two cases differs only in the fourth order in the perturbation theory, resulting in the second term in Eq. (12). The ferromagnetic term there is consistent with the double-exchange idea of Anderson and Hasegawa[25] and of de Gennes,[26] where T_1 can be thought of an effective Mn-Mn hopping, while the expression for T_2 is indicative of the origin of double exchange from simultaneous double hops as originally envisaged by Zener.[27]

As Eq. (12) shows, the net exchange in the d^4-d^4 system can either be ferromagnetic or antiferromagnetic depending on which of the two terms dominates. Indeed in the observed type-A structure for $LaMnO_3$, the exchange is sometimes ferromagnetic (intraplane) and sometimes antiferromagnetic (interplane). The net exchange may be obtained by computing the magnitudes of the hoppings T_1 and T_2 using the parameters in Table I for the different JT-induced orientations of the Mn(e_g) orbitals, viz., e_g, e_g', or e_g''.

Filling in the hopping parameters from Table I, we find that the Mn-O-Mn bond with e_g-e_g configuration has zero exchange,

$$J^{44}(e_g\text{-}e_g) = 0, \tag{15}$$

for all bond angles. This is easily understood by noting that the e_g-e_g configuration allows only electronic hopping from the oxygen to the e_g orbitals (i. e., the z^2-1 orbital pointing along Mn-O bond), which are already occupied in the present case. The hopping to the corresponding x^2-y^2 orbitals to the O(p) orbitals is zero by symmetry, which may be easily seen by considering a new set of O(p) basis states, viz., a p orbital directed along the Mn-O bond, one perpendicular to the plane of the triad, and the third p orbital orthogonal to both these. This is true both for the AF case and the FM case and also whether the t_{2g} hopping is present or not. Consequently, the exchange interaction is zero. This particular type of orbital configuration is however not encountered in $LaMnO_3$.

The configurations encountered in $LaMnO_3$ are the e_g-e_g' configuration, as realized in the (001) planes, and the e_g'-e_g' configuration encountered for two Mn atoms on neighboring planes. For the former case, one finds $T_1=(\sqrt{3}/2)\times t^2\cos(\theta)$ and $T_2=0$, so that Eq. (12) indicates that the exchange is always ferromagnetic,

$$J^{44}(e_g\text{-}e_g')=-\frac{3t^4\cos^2\theta}{4(\Delta_1+\Delta_{JT})^2(U_d+\Delta_{JT})}. \tag{16}$$

The lack of an antiferromagnetic contribution is again due to the suppression of the virtual hopping of the O(p) electron to the unoccupied Mn orbitals because of symmetry and the fact that J_H is large tending to ∞. Note that the sign of the ferromagnetic exchange indicated by Eq. (16) is *independent* of both the electronic parameters as well as the Mn-O-Mn bond angle within our model. Thus the model explains the FM exchange coupling in the ab planes of $LaMnO_3$ and this can be thought of as the Anderson-Hasegawa double exchange arising from the motion of the Mn(d) electrons to the empty d levels. Our model would therefore predict a universal ferromagnetic in-plane coupling provided that the Mn(d^4) atoms occur in the e_g-e_g' configuration.

Next, we turn to the e_g'-e_g' configuration that occurs along the [001] direction in the case of $LaMnO_3$, i.e., where the lobes of neither of the two occupied "z^2-1" orbitals point towards the oxygen. In this case, we find that there is both a FM and an AF contribution, $T_1=(2/\sqrt{3})T_2=(\sqrt{3}/2)t^2\cos\theta$, so that Eq. (12) leads to

$$J^{44}(e_g'\text{-}e_g')=\frac{3t^4\cos^2\theta}{4(\Delta_1+\Delta_{JT})^2}\times\left[-\frac{1}{U_d+\Delta_{JT}}+\frac{3}{2(\Delta_1+\Delta_{JT})+U_p}\right]. \tag{17}$$

The net exchange could be either FM or AF. However, for any reasonable choice of the parameters for the manganites, the exchange turns out to be antiferromagnetic. This is consistent with the interplane AF interaction in $LaMnO_3$.

The exchanges described by Eqs. (16) and (17) are relevant to $LaMnO_3$, where they successfully describe the in-plane ferromagnetic and the interplane antiferromagnetic coupling. The situation with the e_g'' configuration of the Mn atom does not arise in the $LaMnO_3$. However, they may be relevant in other compounds. Within the fourth-order perturbation theory, we find these to be

$$J^{44}(e_g\text{-}e_g'')=J^{44}(e_g\text{-}e_g')$$

and

$$J^{44}(e_g'\text{-}e_g'')=J^{44}(e_g''\text{-}e_g'')=J^{44}(e_g'\text{-}e_g'), \tag{18}$$

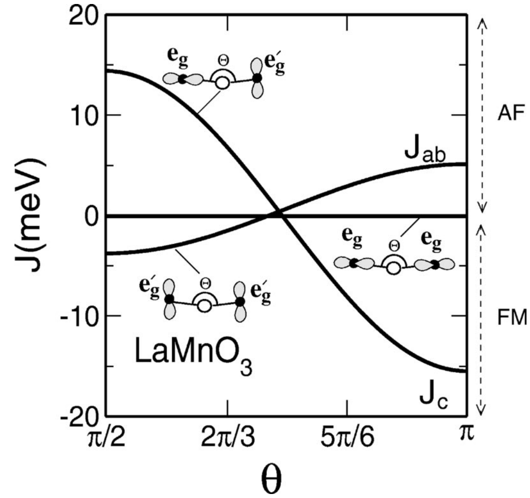

FIG. 10. Exchange interaction in $LaMnO_3$ with the full Hamiltonian, i.e., with $J_H=1$ eV and with t_{2g} hopping included. The intraplane and the interplane exchanges, J_{ab} and J_c, correspond to the e_g-e_g' and e_g'-e_g' orbital orientations, respectively.

where the expressions for $J^{44}(e_g\text{-}e_g')$ and $J^{44}(e_g'\text{-}e_g')$ are given by Eqs. (16) and (17).

In Fig. 9, we show the exchange interaction for $LaMnO_3$ with $J_H=\infty$ calculated from the exact diagonalization, both with and without the t_{2g} hopping. The perturbative results presented above were obtained for the latter case, i.e., with neglect of the t_{2g} hopping. When this coupling is taken into consideration, it adds an extra ferromagnetic component as seen from the figure. The calculated exchanges for $LaMnO_3$ obtained from exact diagonalization are shown in Fig. 9 and they follow the general trend obtained from the results of the perturbation theory.

2. Exchange interaction with the full Hamiltonian

The exchange interactions for the Mn^{3+}-O-Mn^{3+} case appropriate for $LaMnO_3$ are shown in Fig. 10 as calculated from the exact diagonalization of the full Hamiltonian, i.e., with $J_H=1$ eV and with all hoppings including the t_{2g} hopping present. For the straight Mn-O-Mn bond ($\theta=180°$), the intraplane exchange J_{ab} is ferromagnetic and the interplane exchange J_c is antiferromagnetic exactly as observed in $LaMnO_3$. Notice also from the figure that the sign of the exchange is reversed if the Mn-O-Mn bond is bent beyond the value of $\theta\leqslant 135°$ or so. The calculated magnitudes of the J's are compared to the experimental as well as earlier theoretical results in Table III for the compound $LaMnO_3$. The signs of the J's agree with the experimental results as well as with the theoretical results of Su *et al.*[6] obtained from the Hartree-Fock calculations. The magnitudes of the J's are satisfactory compared to the experimental values, given the simplicity of the model and considering the fact that the magnitudes are very sensitive to the strength of the electron hopping.

C. $La_{1/2}Ca_{1/2}MnO_3$

The compound $La_{1/2}Ca_{1/2}MnO_3$ has the peculiar type-CE structure as shown in Fig. 1(c) and here too we find that all exchange interactions are correctly described within our model.

TABLE III. Comparison of the exchange interaction energies J's for $LaMnO_3$ obtained from the present theory with those obtained from Hartree-Fock [Ref. 6] and Density-Functional [Ref. 5] calculations and from inelastic neutron scattering experiments [Ref. 28] in meV.

	Exp.	Present theory	Hartree-Fock approximation	Local spin density approximation
J_{ab}	-13.4	-15.5	-7.0	-18.2
J_c	9.7	5.1	1.7	-6.2

First we consider the interplanar exchange between two Mn atoms on neighboring ab planes in the c direction. There are two types of interplanar coupling, viz., (i) Mn^{4+}-O^{2-}-Mn^{4+} just like in $CaMnO_3$ and (ii) Mn^{3+}-O^{2-}-Mn^{3+} with the e_g'-e_g' orbital orientation like in the case of $LaMnO_3$. Both these cases were discussed in the previous sections and both interactions are antiferromagnetic in agreement with the experiments.

We now turn to the two new situations not discussed above. These correspond to the *intra-planar* exchange in the ab plane, where one of the two Mn atoms has the d^4 configuration while the other has d^3. In one case, the two Mn atoms have the "$d^4(e_g)$-d^3" configuration in accord with the notation described in Fig. 2. The corresponding Mn-O-Mn triads form the ferromagnetic zigzag chains. In the second case, the two Mn atoms that belong to two neighboring zigzag chains have the "$d^4(e_g')$-d^3" configuration and are antiferromagnetically coupled. The zigzag chains are shown by heavy lines in Fig. 1(c).

We have obtained the expressions for the exchange interaction in both these cases by using nondegenerate perturbation theory. At first sight, it might appear that the groundstate is degenerate for the present d^4-d^3 situation, since the lone e_g electron can be on one of the Mn atoms or the other. This would be true if the two Mn sites were equivalent. However, because the octahedral distortion is present around Mn^{3+} but not around Mn^{4+}, symmetry is broken and the ground state is in fact nondegenerate. The results of the perturbation theory for the case of the straight bond ($\theta = 180°$) and neglecting the t_{2g} hoppings are given by

$$J^{43}(e_g\text{-}d^3) = \frac{-t^4}{\Delta_2^2(\Delta_2 + U_d + \Delta_{JT} - \Delta_1)} \tag{19}$$

for the "$d^4(e_g)$-d^3" configuration and

$$J^{43}(e_g'\text{-}d^3) = \frac{t^4}{16}\left[\frac{-1}{\Delta_2^2(\Delta_2 + U_d + \Delta_{JT} - \Delta_1)} + \frac{3}{\Delta_1^2 \Delta_{JT}} + \frac{3(\Delta_1 + \Delta_2)}{\Delta_1 \Delta_2} \times \left(\frac{1}{\Delta_1(\Delta_1 + \Delta_2 + U_p)} + \frac{1}{2\Delta_2 \Delta_{JT}}\right)\right] \tag{20}$$

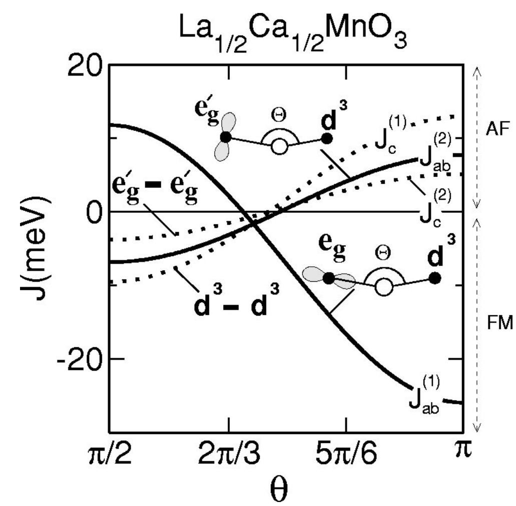

FIG. 11. Calculated exchange for $La_{1/2}Ca_{1/2}MnO_3$ obtained from exact diagonalization of the full Hamiltonian. In the ab plane, there are two different exchange interactions, viz., J_{ab}^1 corresponding to the $d^4(e_g)$-d^3 configuration and J_{ab}^2 corresponding to the $d^4(e_g')$-d^3 configuration. The exchange interactions J_c^1 and J_c^2 between two Mn atoms along the c axis correspond to the d^3-d^3 and $d^4(e_g')$-$d^4(e_g')$ configurations, respectively (see Fig. 1). Results for J_c^1 and J_c^2 are the same as those presented in Figs. 8 and 10.

for the "$d^4(e_g') - d^3$" case. Here Δ_1 and Δ_2 are again the charge transfer energies as defined in Eq. (6). Also, $J_H = \infty$ was used to get the above equations.

The ferromagnetic interaction in Eq. (19) comes from the hopping between the $O(p_z)$ and the $Mn(e_g)$ orbitals. In Eq. (20), the first term describes the same FM interaction except for the reduced magnitude caused by a lower hopping because of the e_g' orientation as opposed to the e_g orientation in the previous case. The remaining three terms originate from hopping to the E_g' orbital, which was missing in the previous case because there the e_g' orbital was involved with zero $O(p_z)$-e_g' hopping. This latter contribution turns out to be antiferromagnetic and it in fact dominates the exchange, producing an overall AF interaction.

In Fig. 11, we show the exchange computed for $La_{1/2}Ca_{1/2}MnO_3$ from exact diagonalization using the full Hamiltonian. These results are consistent with the perturbation theory Eqs. (19) and (20). As seen from the figure, the exchange interaction for the "$d^4(e_g)$-d^3" case is ferromagnetic consistent with the ferromagnetic zigzag chains on the ab plane, while it is antiferromagnetic for the "$d^4(e_g')$-d^3" case, consistent with the AF interchain interaction. Thus, all magnetic exchange interactions are correctly described for the $La_{1/2}Ca_{1/2}MnO_3$ compound.

The calculated exchange interaction and the corresponding experimental values for all three manganites are summarized in Table IV. The calculated signs of J's are robust and agree with experiment in all cases. The calculated magnitudes of J can be brought into perfect agreement with the experiment by taking a slightly different t for each case.

TABLE IV. Comparison of the calculated J's with the experimental values in meV. The calculated values are for the parameters of Table II. In $LaMnO_3$, we define J_{ab} and J_c as the interplane and intraplane exchange interaction energies. In $La_{1/2}Ca_{1/2}MnO_3$, $J_{ab}^{(1)}$ and $J_{ab}^{(2)}$ are defined respectively as the intrachain and interchain exchange interactions in the ab plane and $J_c^{(1)}$ and $J_c^{(2)}$ as the Mn^{4+}-Mn^{4+} and Mn^{3+}-Mn^{3+} exchange interactions in the c direction. The J's for $La_{1/2}Ca_{1/2}MnO_3$ are not known experimentally except for the signs [Ref. 10]. The J's in the Table correspond to the $J^{\mu\nu}$'s in the text as follows: $J=J_c^{(1)}=J^{33}$, $J_{ab}=J^{44}(e_g\text{-}e_g')$, $J_c=J_c^{(2)}=J^{44}(e_g'\text{-}e_g')$, $J_{ab}^{(1)}=J^{43}(e_g\text{-}d^3)$, and $J_{ab}^{(2)}=J^{43}(e_g'\text{-}d^3)$.

	Exchange	Experiment	Theory
$CaMnO_3$	J	13.1 [Refs. 10,24]	13.1
$LaMnO_3$	J_{ab}	−13.4 [Ref. 28]	−15.5
	J_c	9.7 [Ref. 28]	5.1
$La_{1/2}Ca_{1/2}MnO_3$	$J_{ab}^{(1)}$	−	−25.9
	$J_{ab}^{(2)}$	+	7.7
	$J_c^{(1)}$	+	13.1
	$J_c^{(2)}$	+	5.1

IV. RELATIONSHIP WITH ANDERSON-HASEGAWA DOUBLE EXCHANGE

In this section, we clarify the relationship between the analysis presented above and the Anderson-Hasegawa double exchange. Recall that in the standard Anderson-Hasegawa double exchange, the exchange energy goes as $E=-t\cos(\chi/2)$, where χ is the angle between the two Mn core spins taken here as classical spins. In the Anderson-Hasegawa treatment, the t_{2g} spins are treated as classical, core spins with no t_{2g} hopping and $J_H=\infty$. Our discussion in this section pertains to these approximations for the sake of concreteness.

If one extends the model slightly to allow for the two Mn sites to have different energies (differing by V), then following the logic of Anderson-Hasegawa, the exchange energy is easily found to be

$$E(\chi)=-\frac{1}{2}\sqrt{V^2+4t^2\cos^2(\chi/2)}. \tag{21}$$

which goes as $\cos\chi$ instead of $\cos(\chi/2)$ in the limit $t/V\ll 1$.

Our results for the manganites shows the $J\sim t^4$ dependence, even for Mn^{3+}-O-Mn^{4+} where the double-exchange ideas should be appropriate. To clarify the reasons for this, we consider a three-site model keeping only a single nondegenerate orbital on the intermediate atom for simplicity (Fig. 12). The model has three parameters: (i) the Mn-O hopping integral t, (ii) the on-site energy difference between the two Mn sites V, and (iii) the Mn-O charge-transfer energy Δ. We again take the double-exchange limit $J_H\gg t$, so that only one spin state parallel to the classical core spin is accessible.

The Hamiltonian matrix is quite simple since we have just four many-particle configurations: $|1110\rangle$, $|1101\rangle$, $|1011\rangle$, and $|0111\rangle$, with the single-particle occupancies in the order $|O\uparrow\rangle$, $|O\downarrow\rangle$, $|\mathrm{Mn}(\mathit{left})\rangle$, and $|\mathrm{Mn}(\mathit{right})\rangle$. The spins of the Mn sites

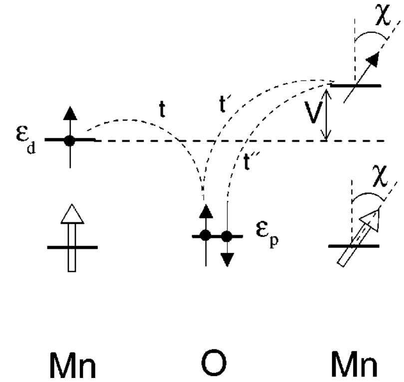

FIG. 12. Three-site model to study the Anderson-Hasegawa double exchange when magnetic interaction is allowed only via hopping to an intermediate atom, with no direct Mn-Mn hopping present. The big arrows indicate the Mn core spins that are treated here as classical spins. Small arrows show the spin orientation of the one-particle states while the dots indicate their occupancies. The hoppings t' and t'' are given by $t'=t\cos(\chi/2)$ and $t''=t\sin(\chi/2)$ following the Anderson-Hasegawa logic.

are fixed by the orientation of the core spins as indicated in Fig. 12. Taking the energy of the first configuration to be ϵ, we have

$$H(\chi)=\begin{pmatrix} \epsilon & 0 & -t\sin(\chi/2) & t\cos(\chi/2) \\ 0 & \epsilon+V & 0 & -t \\ -t\sin(\chi/2) & 0 & \epsilon+V+\Delta & 0 \\ t\cos(\chi/2) & -t & 0 & \epsilon+V+\Delta \end{pmatrix}. \tag{22}$$

The ground-state energy can be obtained by diagonalization, which for $V=0$ is given by

$$E_{gr}(\chi)=\epsilon+\frac{\Delta}{2}-\sqrt{\frac{\Delta^2}{4}+t^2(1+\cos(\chi/2))}. \tag{23}$$

Retaining terms to the lowest order in t, we have

$$E_{gr}(\chi)\approx\epsilon-\frac{t^2}{\Delta}(1+\cos(\chi/2)). \tag{24}$$

The ground-state energy is of the Anderson-Hasegawa form with the effective hopping $t_{eff}=t^2/\Delta$ as one might have expected since hopping takes place via an intermediate atom. In addition, the $\cos(\chi/2)$ form is retained.

For $V\neq 0$, it is tedious to write down the exact ground-state energy. It suffices to obtain the perturbation-theory result,

$$E_{gr}(\chi)\approx\epsilon-\frac{t^2}{(V+\Delta)}+\frac{t^4}{(V+\Delta)^3}-\frac{t^4}{2V(V+\Delta)^2}(1+\cos\chi). \tag{25}$$

Note that the exchange is still ferromagnetic and varies as t^4 (apart from the constant terms that do not depend on the angle χ). In addition we now have the $\cos\chi$ dependence instead of the $\cos(\chi/2)$ dependence obtained for $V=0$. The

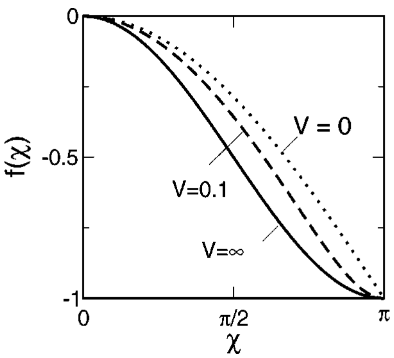

FIG. 13. Dependence of the exchange energy $E(\chi)$ on the relative orientation χ of the Mn core spins calculated from the diagonalization of Eq. (22) for different values of V. Other parameters are $t=1$ eV and $\Delta=5$ eV. Plotted along the y axis is the function $f(\chi)\equiv[E(\chi)-E_\pi]/(E_\pi-E_0)$. Note that the angle dependence changes gradually from the Anderson-Hasegawa $\cos(\chi/2)$ form (dotted line) to the Heisenberg $\cos(\chi)$ form (solid line) as V is varied from 0 to ∞.

t^4 dependence of J for the manganites obtained in the previous sections is similar to what we obtain from Eq. (25). This dependence originates from the fact that the magnetic interaction occurs via an intermediate atom plus the fact that the on-site energies of the two Mn atoms in Mn^{3+}-O-Mn^{4+} are different on account of the Jahn-Teller distortions of the surrounding octahedra.

The angle dependence of the exchange energy $E(\chi)$ obtained from the diagonalization of Eq. (22) is shown in Fig. 13. The figure shows a crossover between the $\cos\chi/2$ and the $\cos\chi$ behavior of the exchange energy as obtained from the perturbation results, Eqs. (24) and (25).

V. CONCLUSION

In summary, we have studied in detail the magnetic exchange interaction between two Mn atoms mediated by the oxygen atom on the Mn-O-Mn triad, taking into account the Jahn-Teller induced orbital orientation of the Mn(e_g) orbitals and the appropriate Mn(d)-O(p) hopping. The magnetic exchange depends very strongly on the valence state of the Mn atoms as well as on the e_g orbital orientation, in such a way that the magnetic structure of all three manganites, viz., $CaMnO_3$, $LaMnO_3$, and $La_{1/2}Ca_{1/2}MnO_3$, are explained in a unified manner within our theory. Figures 8, 10, and 11 and Table IV summarize the calculated exchanges for these three compounds.

Listed in Table II are the Hamiltonian parameters used, which were taken with guidance from earlier density-functional calculations and photoemission experiments. The sign of the exchange is generally insensitive to the Hamiltonian parameters. However, the magnitude of the exchange has a strong dependence on the electronic hopping t, varying as strongly as t^4 in the fourth-order perturbation theory. In view of this, the magnitude of the hopping was fitted to reproduce the measured exchange for $CaMnO_3$, which yielded a reasonable value for the hopping parameter $V_{dd\sigma}=1.65$ eV, as listed in Table II. With these parameters, the calculated exchanges for all three compounds along with the experimental values, wherever known, are listed in Table IV.

We have also considered the effect of the t_{2g} electron hopping on the exchange, an effect often neglected by treating the t_{2g} spin as a localized $S=3/2$ core spin. The effect of retaining the t_{2g} hopping is to add a ferromagnetic contribution to the exchange, which is substantial for a large deviation of the Mn-O-Mn bond from the linear bond. We have shown how this contribution can change the sign of the exchange interaction as a function of the Mn-O-Mn bond angle θ. In the case of $CaMnO_3$, for instance, the exchange interaction changes from antiferromagnetic to ferromagnetic if θ is below a critical value $\theta_c \leqslant 132°$ for the chosen parameters of the Hamiltonian (see Fig. 8). The possibility of such a crossover is long known and recently it has been observed in a somewhat different system $SeCuO_3$.[23]

The effect of the Hund's energy J_H on the exchange was also studied in order to assess the validity of the approximation $J_H\to\infty$, often used in many theoretical works for simplicity. We find that there is a large dependence of the exchange on the magnitude of J_H. In fact, if the $J_H\vec{S}\cdot\vec{\sigma}$ form of the Hund's coupling is used and t_{2g} hopping is neglected, then in the limit of $J_H=0$, magnetic exchange is strictly zero, as the itinerant electrons are not coupled to the t_{2g} core spins. Equation (11) provides an analytical expression for the J_H dependence of the exchange for $CaMnO_3$ (Mn^{4+}-O-Mn^{4+} case), obtained using the fourth-order perturbation theory. From this equation as well as from Figs. 7 and 8, where exchange has been plotted for several values of J_H, it is seen that a finite J_H (~ 1 eV in typical solids) significantly reduces the magnitude of the exchange as compared to the $J_H\to\infty$ value.

In Sec. IV, we discussed the relationship between the Anderson-Hasegawa double-exchange model and our more elaborate model, showing how the familiar double-exchange form $t_{eff}\cos(\chi/2)$ can be recovered from our model as a limit, when one itinerant electron is available to hop between two Mn sites. In the limit that $t<<\Delta$, the effective Anderson-Hasegawa hopping was shown to be given by $t_{eff}=t^2/\Delta$, where t is the Mn-O hopping and Δ is the Mn-O charge-transfer energy. Another interesting result was the finding that the angle dependence of the exchange interaction changes gradually from the Anderson-Hasegawa $\cos(\chi/2)$ form to the Heisenberg $\cos(\chi)$ form as the two Mn sites are made unequal by taking a different value for the energy of the itinerant electron (Figs. 12 and 13).

Finally, we note that even though we have focused our attention on the manganites in this paper, the model and the results presented here form a framework for discussion of the magnetic exchange in a variety of other materials as well.

ACKNOWLEDGMENTS

We thank T. A. Kaplan for stimulating discussions. This work was supported in part by a grant from the Department of Energy under Contract No. DOE FG02-00E0045818.

*Present address: Information Office, ESRF BP2000, 38043 Grenoble, France.

[1] J. B. Goodenough, J. Phys. Chem. Solids **6**, 287 (1958); J. B. Goodenough and A. L. Loeb, Phys. Rev. **98**, 391 (1955).
[2] J. Kanamori, J. Phys. Chem. Solids **10**, 87 (1959).
[3] P. W. Anderson, Phys. Rev. **115**, 2 (1959); in *Magnetism I*, edited by G. T. Rado and H. Suhl (Academic Press, New York, 1963).
[4] J. B. Goodenough, *Magnetic Properties of Perovskites*, Landolt-Bornstein Tabellen, Vol. II, pt. 9 (Springer-Verlag, Berlin, 1962), pp. 2–187.
[5] I. Solovyev, N. Hamada, and K. Terakura, Phys. Rev. Lett. **76**, 4825 (1996).
[6] Y.-S. Su, T. A. Kaplan, S. D. Mahanti, and J. F. Harrison, Phys. Rev. B **61**, 1324 (2000).
[7] S. Satpathy, Z. S. Popović, and F. R. Vukajlović, Phys. Rev. Lett. **76**, 960 (1996); J. Appl. Phys. **79**, 4555 (1996).
[8] Z. S. Popović and S. Satpathy, Phys. Rev. Lett. **84**, 1603 (2000).
[9] W. E. Pickett and D. J. Singh, Phys. Rev. B **53**, 1146 (1996).
[10] E. O. Wollan and W. C. Koehler, Phys. Rev. **100**, 545 (1955).
[11] J. B. Goodenough, Phys. Rev. **100**, 564 (1955).
[12] J. B. Goodenough, *Magnetism and Chemical Bond* (Interscience, New York, 1963).
[13] K. I. Kugel and D. I. Khomskii, Sov. Phys. Usp. **25**, 231 (1982).
[14] S. Ishihara, J. Inoue, and S. Maekawa, Phys. Rev. B **55**, 8280 (1997).
[15] J. C. Slater and G. F. Koster, Phys. Rev. **94**, 1498 (1954).
[16] W. A. Harrison, in *Electronic Structure and the Properties of Solids* (Freeman, San Francisco, 1980).
[17] A. E. Bocquet, T. Mizokawa, T. Saitoh, H. Namatame, and A. Fujimori, Phys. Rev. B **46**, 3771 (1992).
[18] J. H. Jung, K. H. Kim, D. J. Eom, T. W. Noh, E. J. Choi, J. Ju, Y. S. Kwon, and Y. Chung, Phys. Rev. B **55**, 15 489 (1997).
[19] G.-M. Zhao, K. Conder, H. Keller, and K. A. Müller, Nature (London) **381**, 676 (1996); I. Isaac and J. P. Franck, Phys. Rev. B **57**, 5602 (1998).
[20] V. Z. Kresin and S. A. Wolf, Philos. Mag. B **76**, 241 (1997).
[21] S. Satpathy, J. Phys.: Condens. Matter **10**, L501 (1998); H. Meskine and S. Satpathy, J. Appl. Phys. **85**, 4346 (1999); S. Satpathy, Solid State Commun. **112**, 195 (1999).
[22] A. J. Millis, Phys. Rev. B **55**, 6405 (1997).
[23] M. A. Subramanian, A. P. Ramirez, and W. J. Marshall, Phys. Rev. Lett. **82**, 1558 (1999).
[24] G. S. Rushbrooke, G. S. Baker, Jr., and P. J. Wood, in *Phase Transitions and Critical Phenomena*, edited by C. Domb and M. S. Green (Academic Press, London, New York, 1974), Vol. 3, Eqs. (1.1) and (5.4).
[25] P. W. Anderson and H. Hasegawa, Phys. Rev. **100**, 675 (1955).
[26] P.-G. de Gennes, Phys. Rev. **118**, 141 (1960).
[27] C. Zener, Phys. Rev. **82**, 403 (1951).
[28] K. Hirota, N. Kaneko, A. Nishizawa, and Y. Endoh, J. Phys. Soc. Jpn. **65**, 3736 (1996).